

R. M. Gilgenbach, L. D. Horton, R. F. Lucey, Jr,
S. Bidwell, M. Cuneo, J. Miller, and L. Smutek

Intense Energy Beam Interaction Laboratory
Nuclear Engineering Department
The University of Michigan
Ann Arbor, Michigan 48109

Abstract

Experiments have been conducted on the Michigan Electron Long Beam Accelerator (MELBA) to explore diode closure and voltage compensation during collapsing diode impedance. MELBA operates with parameters: Voltage = - 0.6 to -1.0 MV; Current < 60 kA; and Pulselengths exceeding 1 μ s. A reverse charged ringing circuit compensates the Marx generator output voltage to within $\pm 7\%$ ($\pm 10\%$) for pulselengths of 1 μ s (1.4 μ s) in a 127 ohm resistive load. Electron beam generation experiments have utilized two types of field emission cathodes: carbon brush and velvet cloth. Total electron beam pulselengths of 4 μ s have been achieved. Voltage compensation is limited by current spikes to $\pm 13\%$ ($\pm 5\%$) over the first 1 μ s (0.7 μ s). Diode impedance and perveance have been characterized as a function of time at several A-K gap spacings. Current densities have been in the range from 10 to 200 A/cm². The current shows an initial step with a rapid increase at 0.6 to 0.8 μ s followed by either current runaway or a return to Child-Langmuir. Apertured electron beam current shows a similar behavior with large amplitude beam fluctuations during enhanced current. Apparent plasma closure velocities inferred from diode impedance data indicate closure velocities from 3.3 to 6.2 cm/ μ s dependent upon the cathode type. The effective closure velocity, defined by the time required to short circuit the A-K gap, ranges from 2.1 to 4.1 cm/ μ s. Electron beam uniformity and beam dynamics have been investigated by means of apertured anodes with lucite plate diagnostics. Voltage compensation has been tested by comparing experimental voltage traces to transient circuit computer codes with empirical impedance profiles.

Introduction

Most research concerning intense, pulsed electron beams has utilized pulselengths in the range from tens to hundreds of ns. This was due in part to specific applications, (such as inertial confinement fusion), which require short, intense, pulses of energy.

Accelerator size and cost can be reduced when large delivered energies are generated by increasing the beam pulselength rather than the voltage and current. Earlier experiments [1-8] have generated intense, microsecond electron beams by means of Marx generators with pulse forming lines (PFL) or pulse forming networks (PFN). In this article we demonstrate microsecond electron beam generation and voltage compensation with a Marx generator coupled to an Abramyan type RLC ringing, reverse-charged stage [9, 10].

The advantages of the Abramyan circuit over Marx generators with PFLs or PFNs are:

- 1) It requires fewer circuit elements, thus providing more compact, less expensive generators,
- 2) Compensation for different load impedances can be changed by adjusting the relative charging voltages rather than by changing PFN circuit elements,
- 3) The Marx generator directly drives the load, so the voltage requirement is lowered.

Intense electron beams with pulselengths exceeding 1 μ s have a number of important applications:

- 1) Pumping of lasers in the visible, uv, and (possibly) X-ray regime [4,10],
- 2) High power microwave and millimeter wave generators and free electron lasers [11],
- 3) Fusion plasma startup, heating, and stabilization,
- 4) Pulsed X-ray radiography, and
- 5) Rapid heating of materials and gases.

Each of these applications imposes different constraints on the cathode current density and voltage flatness. Electron beam pumped lasers might require a current density on the order of 30 A/cm², whereas high power microwave generators operating in the collective regime may need kA/cm².

Explosive emission cathodes [1-16] have generally been employed in these applications because of their high current densities and immunity to the hostile plasma chemistry environment which poisons thermionic cathodes. This presents a problem in the generation of microsecond electron beams because of the rapid closure of the anode-cathode (A-K) gap by the cathode plasma. According to the Child-Langmuir current scaling, this gap closure causes an increase in the electron current density by the factor $(d - ut)^{-2}$; where d is the initial A-K gap spacing and u is the closure velocity. Another problem intricately related to this increasing current is the maintainance of a flat output voltage throughout the μ s pulse. Constancy of the beam voltage is particularly important for microwave generators which must satisfy resonance conditions. The plasma closure velocity is therefore crucial in determining diode impedance collapse, voltage droop, and A-K gap shorting.

MELBA Design and Performance

The Michigan Electron Long Beam Accelerator (MELBA) was designed [17] to generate 10 kA, 1 MV electron beams into a collapsing diode impedance for 1 μ s pulselengths. The design utilizes an electrical voltage compensation circuit first proposed by Abramyan [9] and later by Smith [10]. This circuit

Report Documentation Page

Form Approved
OMB No. 0704-0188

Public reporting burden for the collection of information is estimated to average 1 hour per response, including the time for reviewing instructions, searching existing data sources, gathering and maintaining the data needed, and completing and reviewing the collection of information. Send comments regarding this burden estimate or any other aspect of this collection of information, including suggestions for reducing this burden, to Washington Headquarters Services, Directorate for Information Operations and Reports, 1215 Jefferson Davis Highway, Suite 1204, Arlington VA 22202-4302. Respondents should be aware that notwithstanding any other provision of law, no person shall be subject to a penalty for failing to comply with a collection of information if it does not display a currently valid OMB control number.

1. REPORT DATE JUN 1985	2. REPORT TYPE N/A	3. DATES COVERED -			
4. TITLE AND SUBTITLE Microsecond Electron Beam Diode Closure Experiments		5a. CONTRACT NUMBER			
		5b. GRANT NUMBER			
		5c. PROGRAM ELEMENT NUMBER			
6. AUTHOR(S)		5d. PROJECT NUMBER			
		5e. TASK NUMBER			
		5f. WORK UNIT NUMBER			
7. PERFORMING ORGANIZATION NAME(S) AND ADDRESS(ES) Intense Energy Beam Interaction Laboratory Nuclear Engineering Department The University of Michigan Ann Arbor, Michigan 48109		8. PERFORMING ORGANIZATION REPORT NUMBER			
9. SPONSORING/MONITORING AGENCY NAME(S) AND ADDRESS(ES)		10. SPONSOR/MONITOR'S ACRONYM(S)			
		11. SPONSOR/MONITOR'S REPORT NUMBER(S)			
12. DISTRIBUTION/AVAILABILITY STATEMENT Approved for public release, distribution unlimited					
13. SUPPLEMENTARY NOTES See also ADM002371. 2013 IEEE Pulsed Power Conference, Digest of Technical Papers 1976-2013, and Abstracts of the 2013 IEEE International Conference on Plasma Science. Held in San Francisco, CA on 16-21 June 2013. U.S. Government or Federal Purpose Rights License.					
14. ABSTRACT Experiments have been conducted on the Michigan Electron Long Beam Accelerator (MELBA) to explore diode closure and voltage compensation during collapsing diode impedance. MELBA operates with parameters: Voltage = - 0.6 to -1.0 MV; Current < 60 kA; and Pulselengths exceeding 1 ps. A reverse charged ringing circuit compensates the Marx generator output voltage to within : 7 % (! 10%) for pulselengths of 1 ps (1.4 ps) in a 127 ohm resistive load. Electron beam generation experiments have utilized two types of field emission cathodes: carbon brush and velvet cloth. Total electron beam pulselengths of 4 ps have been achieved.					
15. SUBJECT TERMS					
16. SECURITY CLASSIFICATION OF:			17. LIMITATION OF ABSTRACT SAR	18. NUMBER OF PAGES 7	19a. NAME OF RESPONSIBLE PERSON
a. REPORT unclassified	b. ABSTRACT unclassified	c. THIS PAGE unclassified			

employs a Marx generator coupled to a ringing RLC circuit.

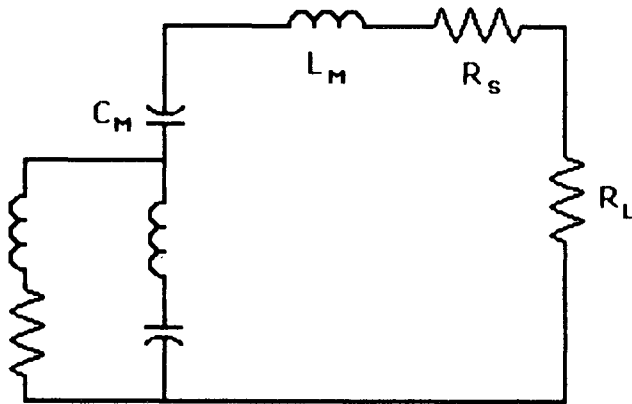


Fig. 1. Simplified schematic of the Abramyan circuit with all spark gap switches closed [9,10]. Not shown are the Marx/switch resistances. The MELBA design also includes a small RC filter circuit on the output. The ringing stage (RS) is charged to initially deliver a voltage of the opposite polarity from the Marx output. At a later time, the polarity of the RS is in the same sense as the Marx output. Separate charging supplies are utilized for the Marx generator and the ringing stage. This allows the amount of voltage compensation to be changed by choosing the relative charging voltage of the Marx versus the ringing stage. The spark gap switches in the Marx generator and the RS are independently triggered; in these experiments the two circuits were triggered simultaneously. MELBA utilizes 14 capacitors in the Marx generator and 2 capacitors in the RS, one third the number of capacitors used in other microsecond electron beam generators [2,3].

Data in Fig. 2 represent a -1 MV output voltage from the MELBA machine into a low inductance 127 ohm resistive load; also shown is the output of the SPICE transient circuit analysis code [18] to illustrate the effect of the ringing, reverse-charged stage.

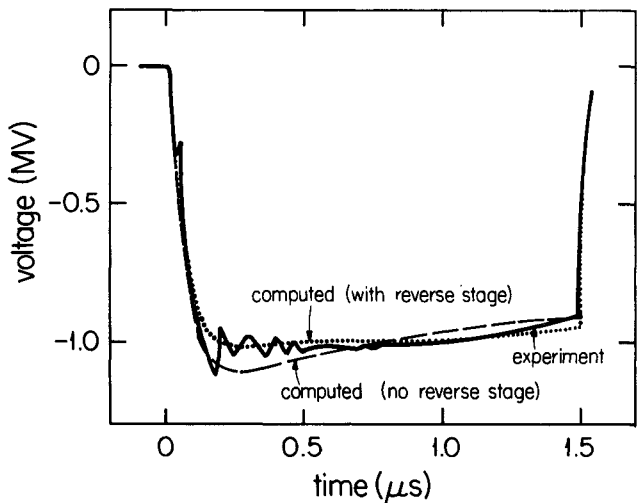


Fig. 2. MELBA output voltage into 127 ohm resistive load.

From the above data it can be seen that the experimental voltage remains flat to within $\pm 7\%$ ($\pm 10\%$) over pulselengths of $1\ \mu\text{s}$ ($1.4\ \mu\text{s}$). The transient circuit code gives excellent agreement with experimental data. It should also be noted from the computer model that without the ringing stage, the voltage would not be flat but would exhibit the RC decay characteristic of Marx rundown circuits.

The generator was constructed with a triggered, high pressure SF₆ crowbar switch to short circuit the generator output after the design pulselength of $1\ \mu\text{s}$. The crowbar switch removed 90% of the generator voltage in about 40 ns. Figure 3 gives the output voltage and current into a resistive load without crowbar firing.

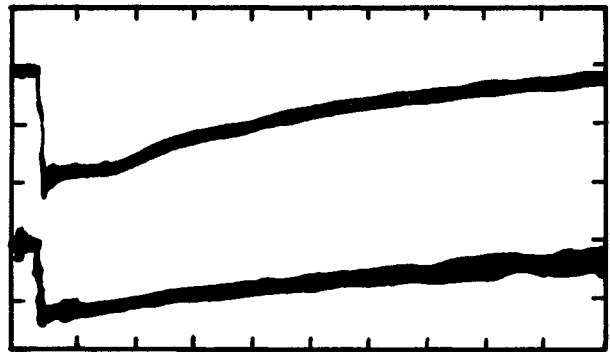


Fig. 3. Voltage (upper, 400 kV/div) and current (lower) into 127 ohm resistive load without crowbar firing (1μs/div). Charging voltages: $V_M = + 56\ \text{kV}$; $V_R = + 54\ \text{kV}$.

The data of Fig. 3 demonstrate the effectiveness of the RS in generating flat voltage out to $1.4\ \mu\text{s}$. The fact that voltage remains on the load for about $10\ \mu\text{s}$ into a resistive load is important for comparison with the electron beam diode closure experiments. The resistor in series with the cathode (Fig. 1) dissipates the stored generator energy in the event of a crowbar or A-K short circuit. This feature permitted experiments to be performed without firing the crowbar in order to investigate plasma closure and shorting with multimicrosecond pulselengths.

Cathode - Anode Configuration

The anode-cathode geometry is depicted in Fig. 4.

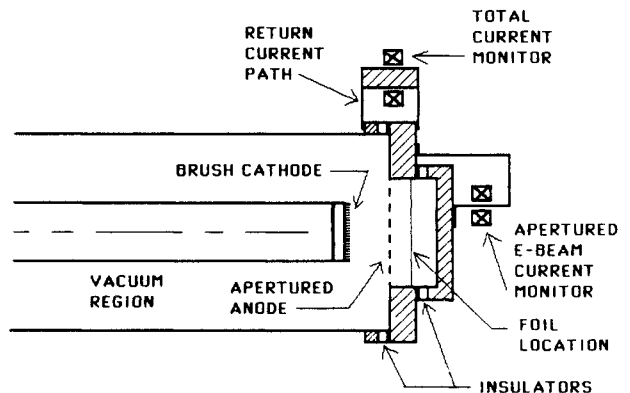


Fig. 4. Anode-cathode configuration.

Since the objective of these experiments was to investigate high current electron beams with multimicrosecond pulse lengths, the anode-cathode spacings were relatively large: 10 cm for most shots, although 8 cm and 6 cm were also used. In order to extract multi-kiloampere currents, two types of large area field emission cathodes were employed in these experiments:

- 1) carbon brush cathode, and
- 2) velvet cloth cathode.

The brush cathode was constructed following the design of Refs. 4 and 11. Carbon string was threaded through a square array of holes on 1 cm centers in a 7 cm radius aluminum plate. The outer radius of the carbon brush array was 6 cm. A smaller (2.5 cm radius) brush cathode was also constructed with recessed CR-39 ion track film to detect ions crossing the A-K gap.

The velvet cathode used in these experiments was 65 % cotton and 35 % rayon. A 6 cm radius circle of this cloth was epoxied to a 7 cm radius aluminum cathode plate.

In both cases, the cathode plate was threaded to the anodized cathode stalk of radius 7 cm. Anode-cathode spacings were adjusted by installing anodized rings between the cathode stalk and the cathode plate.

An extremely durable anode design was required, since the generator was typically operated in a noncrowbarred mode in which plasma shorting of the A-K gap occurred. For this reason it was not possible for foil anodes (or even solid molybdenum anodes) to survive the high current discharge from the capacitor bank after A-K shorting. The high current discharge was much more damaging to anode materials because high current densities deposit energy at the surface, removing material in a vacuum arc mechanism [19]. It was found that a (3.2 mm thick) Poco-graphite anode produced the least contamination of the cathode and insulators for shorted A-K gaps.

The anode plate was insulated from the vacuum tank and up to 6 current transformers were utilized to monitor total return current which passed through low inductance straps. Current signals were summed in the Faraday cage by ferrite adders. Electron beam current was sampled by an array of small (1.6 mm) holes in the graphite anode plate. A beam collector and current transformer permitted measurements of apertured electron beam current. Energy discrimination of apertured electron beam current could be performed by installing foil between the carbon anode and the beam collector. For studies of electron beam uniformity and beam dynamics the electron beam collector was replaced by a lucite plate. The inside of this plate was coated by an opaque layer of Aerodag graphite spray; the outside of this plate was viewed by either an open shutter or streak camera.

Electron Beam Generation Experiments

Brush cathode turn-on data is presented in the voltage and current traces of Figure 5.

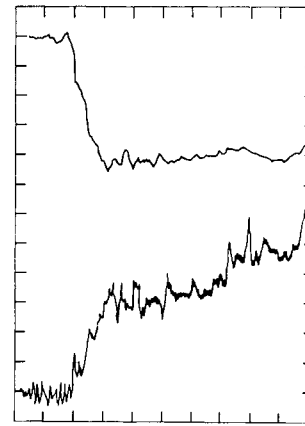


Fig. 5. Cathode turn-on data for carbon brush with 10 cm A-K gap. (100 ns/div)
Upper trace: Voltage (160 kV/div)
Lower trace: current (2.28 kA/div)

The initial detectable current always coincided with the knee (at about 30 ns) during the rise of generator voltage. Rapid current fluctuations were measured for both types of cathodes. The spiky nature of the current agrees with the NRL induction linac results in which a similar brush cathode was compared with a thermionic cathode [11]. The cause of the current fluctuations could be nonsimultaneity in the explosive emission from the multiple tufts of carbon string. Voltage compensation at early times is seen to be excellent, with flat voltage ($\pm 5\%$) over a $0.7 \mu\text{s}$ pulse.

Electron beam uniformity was measured by means of the lucite plate diagnostic. Figure 6 gives an open shutter photograph of the lucite plate for a MELBA pulse which crowbarred at $0.5 \mu\text{s}$.

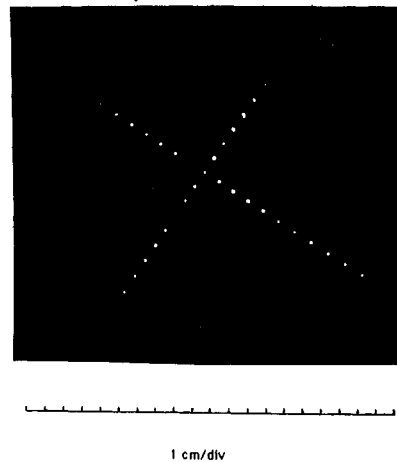


Fig. 6. Open shutter photograph of lucite plate for $0.5 \mu\text{s}$ electron beam pulse. Brush cathode with 10 cm A-K gap.

The lucite plate data indicates that the electron beam has good uniformity over the full cathode diameter. For longer electron beam pulses, the large electrostatic charge deposited in the lucite caused arcing between the apertured beamlets, obscuring the data and damaging the lucite.

Diagnostic data for two noncrowbarred electron beam pulses from MELBA are presented in Fig. 7.

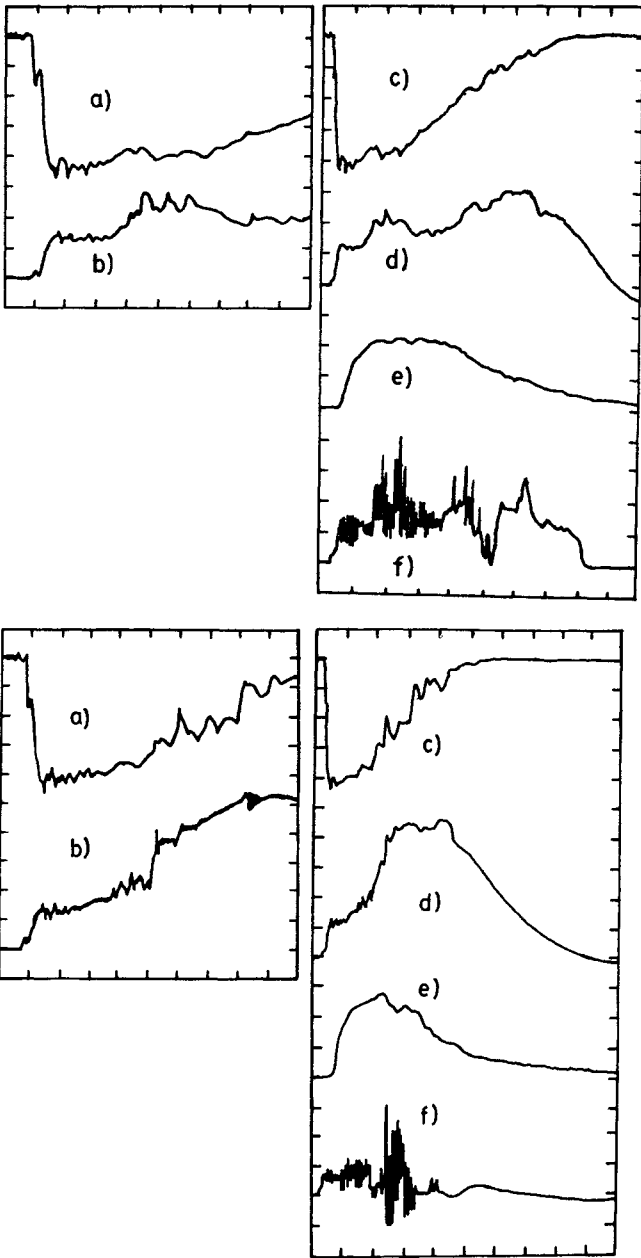


Fig. 7 MELBA electron beam pulse without crowbar, upper data represent Type A shot; lower data set represents Type B shot.

- a) Voltage (160 kV/div; 0.2 μ s/div)
- b) Current (5.3 kA/div; 0.2 μ s/div)
- c) Voltage (160 kV/div; 0.5 μ s/div)
- d) Current (6.2 kA/div; 0.5 μ s/div)
- e) Hard X-rays (0.5 μ s/div)
- f) Apertured e-beam current (20 A/div, 0.5 μ s/div), no foil.

Parameters: Brush cathode on 7 cm radius plate, A-K gap of 10 cm. Charging voltages: $V_m = \pm 56$ kV and $V_r = \pm 56$ kV

Two types^m of current behavior were observed: Type A with flat or decreasing current late in the pulse, and Type B with current continually increasing throughout the pulse. For brush and velvet cathodes, the voltage flatness was limited by large current spikes and the rapid increase which typically occurred.

Large current spikes are believed to be cathode flares from individual tips and were also observed in lower current density Soviet experiments. The apertured e-beam signal exhibited large fluctuations during enhanced current. These large current fluctuations could be caused by a streaming instability. [20]

Diode Closure Velocities

For purposes of this research it is useful to define two closure velocities: 1) The effective closure velocity v , is defined by the shorting time of the A-K gap. 2) Apparent closure velocity u , is that which is defined in terms of the Child-Langmuir current with a closing A-K gap; it is obtained from the slope of $(P)^{-1/2}$, where P is the perveance.

The data of the Type A shot in Fig. 7 shows that the voltage, hard X-rays, and apertured e-beam current persist for 3.7 μ s with a 10 cm A-K gap; this yields an effective closure velocity of 2.7 cm/ μ s.

Figure 8 gives the time history of the diode impedance and $(P)^{-1/2}$, for the same two shots given in Fig. 7.

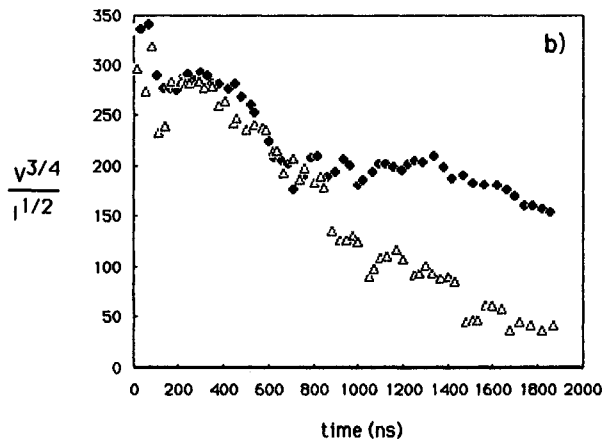
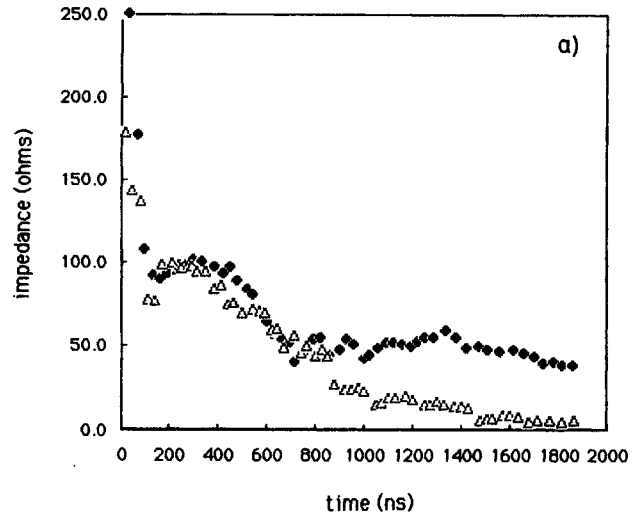


Figure 8. Temporal evolution of data from Fig. 7: a) Impedance profile for type A shot (solid points) and type B shots (open points), b) $P^{-1/2}$

Note that type A shots gave a flat impedance (50 ohms) after about 0.8 μ s whereas type B shots gave continually drooping impedance. In type A shots the slope of $P^{1/2}$ appears to change at about 0.8 μ s. This has been interpreted by others as an actual slowing of the cathode plasma velocity by "electric pressure" [21] or by the beam magnetic field [22]. For a 10 kA beam current the magnetic pressure is much less than the kinetic pressure of typical cathode plasma. However, the relativistic Child-Langmuir analysis of the next section shows that the type A current can be modeled by a constant closure velocity at early and late times.

Table 1 summarizes the apparent and effective diode closure velocities for brush and velvet cathodes at different A-K gap spacings.

Table 1

Summary of Diode Closure Velocities (cm/ μ s)

A-K gap(cm)	BRUSH		VELVET	
	10	8	10	8
Apparent				
Type A	3.3 \pm .4 (3)	3.3 (1)	None	
Type B	5.3 \pm .4 (2)	6 (1)	6.1 (1)	6.2 (1)
Effective				
Type A	3 \pm .7 (3)	2.1 \pm .3 (7)	None	
Type B	3.5 \pm .6 (4)	2.6 (1)	3 \pm .6 (4)	4.1 \pm .3 (5)

(Numbers in parentheses indicate shots averaged)

It should be noted that the velvet cathodes always gave continually increasing current (type B) behavior. In spite of the higher electric field a number of brush cathode shots with $d_{ak} = 8$ cm demonstrated lower closure velocities than the same cathode with $d_{ak} = 10$ cm.

Diode Current Data and Modeling

Our model for current flow from a moving source plasma in the diode employs a fully relativistic version of the Child-Langmuir current density which can be modified by the inclusion of ion flow [23]. Following the technique of Poukey, we perform a Romberg integration solution for the current density corresponding to space charge potentials in a planar diode gap. For our model we have also included closure of the A-K gap by the cathode plasma with velocity u and ion flow of variable magnitude [23-25]. Edge emission was modeled by the technique of Parker [26].

Two types of temporal current behavior were observed in these experiments. Figure 9 compares type A and type B current traces with theoretical models.

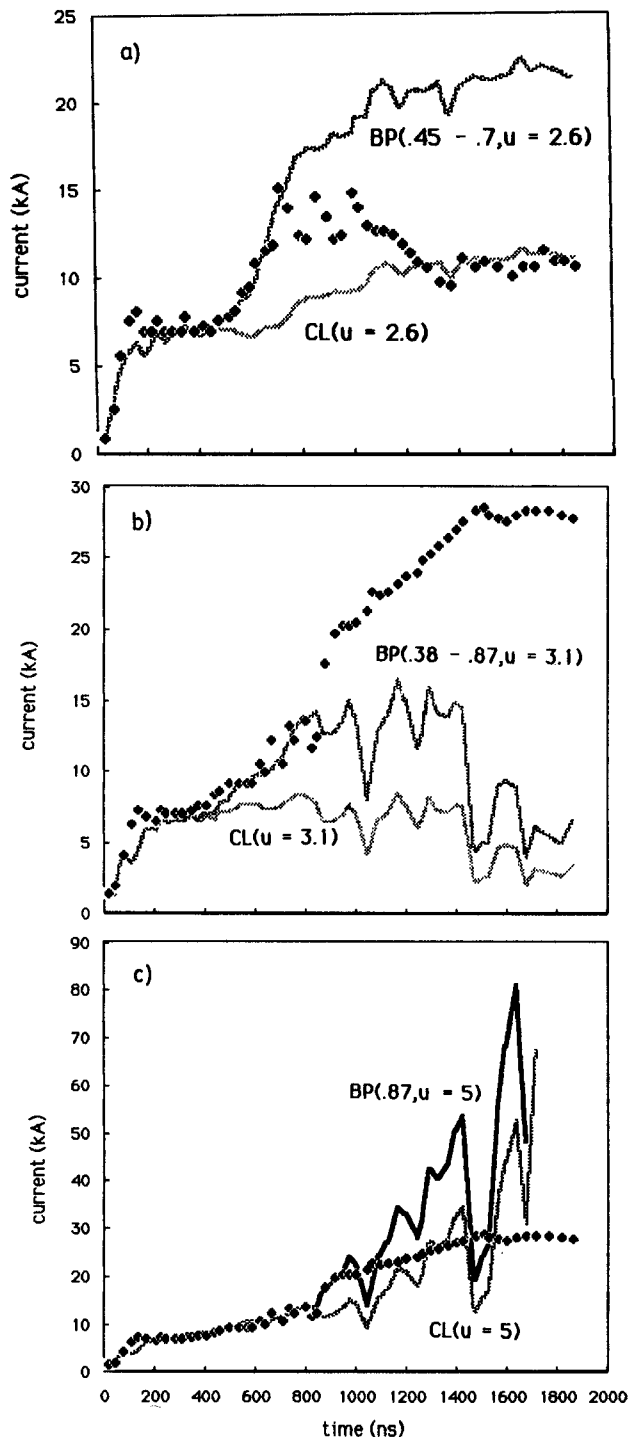


Fig.9 a) Experimental current data (points) from type A shot compared with constant closure velocity model ($u = 2.6$ cm/ μ s) for Child-Langmuir (CL) current and bipolar flow (BP) turned on linearly from 0.45 μ s to 0.7 μ s.

b) Experimental current data from type B shot compared to Child-Langmuir (CL) with closure velocity of 3.1 cm/ μ s and bipolar (BP) flow turned on linearly from 0.38 μ s to 0.87 μ s with constant closure velocity.

c) Experimental current data from type B shot compared to Child-Langmuir (CL) with a constant closure velocity of 5 cm/ μ s and bipolar flow (BP) turned on at 0.87 μ s.

Note from Fig. 9a that the experimental current agrees with the Child-Langmuir model from 0 to 0.45 μsec and from 1.2 μs to 1.9 μs . However, between 0.45 μs and 0.7 μs , a linear transition to bipolar flow models the data very well. A physical explanation for the type A current behavior is that at early times (less than 0.45 μs) the cathode emits the Child-Langmuir current. Between 0.6 μs and 0.7 μs ions from the anode or the background gas ($3 - 8 \times 10^{-5}$ Torr) are sufficient to support bipolar flow. At later times (greater than 0.7 μs) "ion starvation" causes the current to return to Child-Langmuir flow.

In type B shots the early time behavior is similar to type A. The type B shots, however, exhibit continually increasing current throughout the pulse. Figure 9b shows that even a transition to bipolar flow (at constant closure velocity) cannot model this rapid current increase. An increased closure velocity of 5 cm/ μs , modeled in Fig. 9c, would provide a physical mechanism for the rapid current increase. This agrees with Ref. 27 in which the authors conclude that for cases in which a threshold energy dose rate is exceeded, the anode plasma gives both a transition to bipolar flow and an increased diode closure velocity. It should be noted that the energy density to the anode in our experiments is near the required 400-600J/g dose for graphite [27]. The longer pulselengths in our experiments may reduce the threshold energy for anode plasma production. For microsecond pulselengths it is also possible that background gases play a role in ion production.

The interpretation of enhanced current in terms of anode plasmas is supported by the observation that the apertured e-beam signal always showed enhanced fluctuation levels during the period of increasing current. These large fluctuations could be indicative of a streaming interaction between the beam and the anode plasma [20]. Etching of the CR-39 track film embedded in a cathode gave a crater over the entire exposed area suggesting a large flux of low energy ions backstreaming to the cathode.

Some additional observations concern the conditions under which type A and type B currents were measured. Velvet cathodes always gave type B current. For 8 cm A-K gaps the brush cathode was more likely to give type A behavior (7 out of 8 shots).

Brush cathode experiments with 10 cm A-K gaps showed that on the first several shots after opening the diode to air, a type A shot was more likely; on later shots a type B shot was more likely. Apparently the cathode current density, surface chemistry and residual gas play a role in microsecond plasma production.

Transient Circuit Codes and Voltage Compensation

The generator system performance was calculated with the SPICE transient circuit analysis program. The computational model includes stray capacitances, inherent inductance loops, effective Marx shunt impedance, and the RC filter circuit. The

values of the various elements were derived by PSI [17] from a combination of measurements, experimental data, extrapolations, and calculations. The SPICE circuit code has been run for fixed resistance loads as well as time varying impedances. For the time-varying diode impedance, the load is modeled in a piecewise linear manner using a nonlinear circuit element (typically a JFET).

Current spikes and irreproducibility in the diode current made direct experimental comparison of different compensating voltages difficult on separate shots.

Figure 10 compares the experimental voltage with transient circuit analysis code results using the experimental impedance profile for two cases:

- 1) Actual MELBA circuit and charging voltages, and
- 2) MELBA circuit but increased charging voltage of ringing stage.

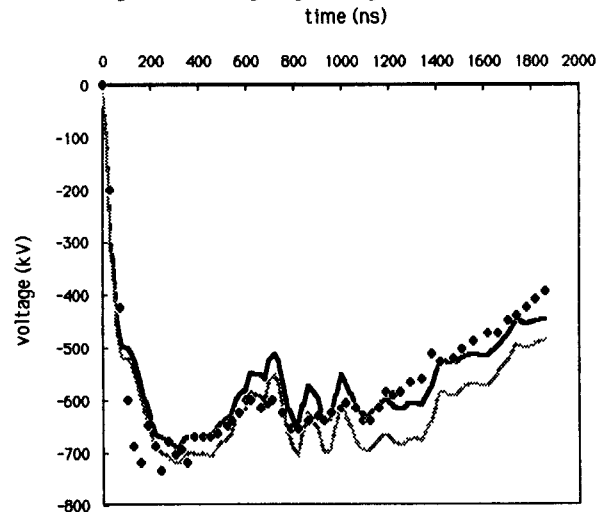


Fig. 10. MELBA experimental voltage (points) for type A shot compared to SPICE code using experimental impedance profile with: Actual charging voltages (dark line) $V_M = +56$ kV, $V_R = +56$ kV, and, increased charging voltage on the reversed stage, $V_M = +56$ kV, $V_R = +90$ kV

It can be seen that increasing the ringing reverse stage charging voltage improves the voltage flatness between 0.8 μs and 1.4 μs . However, the voltage deviations observed in these experiments have been caused primarily by current spikes and the rapid current enhancement starting at 0.45 μs . Current spikes may be eliminated by resistively ballasting the individual emitters on a multitip or brush cathode.

*Supported by ONR, NSF and GM Research Labs
References

- 1) H. Friedman and M. Ury, "Microsecond duration intense relativistic electron beams," The Review of Scientific Instruments, Vol. 43, No. 11, pp. 1659-1661, August 9, 1972.
- 2) T. H. Martin and R. S. Clark, "Pulsed microsecond high-energy electron beam accelerator," The Review of Scientific Instruments, Vol. 47, No. 4, pp. 460-463, April 1976.

- 3) R. Schneider, C. Stallings, and D. Cummings, "Generation and extraction of microsecond intense relativistic electron beams," Journal of Vacuum Science Technology, Vol. 12, No. 6, pp. 1191-1193, Nov./Dec. 1975.
- 4) Juan J. Ramirez and Donald L. Cook, "A study of low-current-density microsecond electron beam diodes," Journal of Applied Physics, Vol. 51, No. 9, pp. 4602-4611, September 1980.
- 5) M. A. Vasilevskii, I. M. Roife, and V. I. Engel'ko, "Operating characteristics of explosive-emission multipoint cathodes with microsecond pulse lengths," Zh. Tekh. Fiz. 51, 1183-1194 (Soviet Journal of Technical Physics, Vol. 26, No. 6, pp. 671-678), June 1981.
- 6) V. S. Noronin, S. M. Zakharov, L. N. Kazanskii, and S. A. Pikuz, "Intense monoenergetic microsecond electron beam with stabilized current," Pis'ma Zh. Tekh. Fiz. 7, 1224-1227 (Soviet Technical and Physical Letters, Vol. 7, No. 10, pp. 523-524), October 1981.
- 7) S. V. Lebedev, V. V. Chikunov, and M. A. Shcheglov, "Microsecond-length relativistic electron beams from a plane diode," Pis'ma Zh. Tekh. Fiz. 8, 693-696 (Soviet Technical and Physical Letters, Vol. 8, No. 6, pp. 302-303), June 1982.
- 8) V. A. Burtsev, M. A. Vasilevskii, O. A. Gusev, I. M. Roife, E. V. Seredenko, and V. I. Engel'ko, "High-current relativistic electron beam with length greater than 10^{-5} sec," Pis'ma Zh. Tekh. Fiz. 2, 1123-1126 (Sov. Tech. Phys. Lett., Vol. 2, No. 12, pp. 441-442), December 1976.
- 9) E. A. Abramyan, E. N. Efimov, and G. D. Knieshav, "Energy recovery and power stabilization of pulsed electron beams in Marx generator circuits," in Proceedings of the 2nd International Topical Conference on High Power Electron and Ion Beam Research and Technology, Vol. 2, Oct. 3-5, 1977, pp. 755-760.
- 10) Ian Smith, "Pulse power for 0.3-0.5 us. durations," Lawrence Livermore Laboratory Report, UCID - 18318, October 1979.
- 11) C. W. Roberson, J. A. Pasour, F. Mako, R. F. Lucey, Jr., and P. Strangle, "A free-electron laser driven by a long-pulse induction linac," Infrared and millimeter waves, Vol. 10, Academic Press, Inc., 1983, Ch. 7, pp. 361-397.
- 12) R. Prohaska and A. Fisher, "Field emission-cathodes using commercial carbon fibers," Rev. Sci. Instrum., Vol 53, No. 7, pp. 1092-1093, July 1982.
- 13) E. N. Abdullin, G. P. Bazhenov, S. P. Bugaev, and O. B. Ladyzhenskii, "Formation of millisecond electron beams through explosive electron emission," Pis'ma Zh. Tekh. Fiz. 7, 347-350 (Sov. Tech. Phys. Lett., Vol. 7, No. 3, pp. 148-149), March 1981.
- 14) Yu. A. Vasilevskaya, M. A. Vasilevskii, I. M. Roife, V. I. Engel'ko, S. P. Yakovlev, and E. G. Yankin, "Electron beam formation in a diode with a multiple-tipped explosive emission cathode," Zh. Tekh. Fiz. 53, 677-682 (Sov. Phys. Tech. Phys. Vol. 28, No. 4, pp. 429-432), April 1983.
- 15) G. P. Bazhenov, S. P. Bugaev, G. A. Mesyats, and S. M. Chesnokov, "Use of explosive emission to produce current pulses longer than 10^{-4} sec," Pis'ma Zh. Tekh. Fiz. 2, 462-465 (Sov. Tech. Phys. Lett., Vol. 2, No. 5, pp. 180-181), May 1976.
- 16) V. A. Burfsev, M.A. Burfsev, M. A. Vasilevskii, I. M. Roife, E. V. Seredenko, and V. I. Engel'ko, "Improved stability of explosive-emission multiple-tip cathodes," Pis'ma Zh. Tekh. Fiz. 4, 1083-1087 (Sov. Tech. Phys. Lett. Vol. 4, No. 9, pp. 436-37), September 1978.
- 17) Phillip Champney, "Electron beam accelerator," Pulse Sciences Inc. Proposal: PSI-P-83-105, August 1983.
- 18) E. Cohen, A. Vladimirescu, D. O. Pederson, "User's guide for SPICE circuit simulation program," Univ. of Calif., Berkeley.
- 19) V. A. Nemchinskii, "Anode spot in a high-current vacuum arc," Zh. Tekh. Fiz. 52, 35-42 (Sov. Phys. Tech. Phys. Vol. 27, No. 1, pp. 20-25), January 1982.
- 20) R. J. Briggs, "Electron Stream Interaction with Plasmas," Research Monograph No. 29, MIT Press, Cambridge, MA., 1964.
- 21) D. D. Hinshelwood, "Explosive Emission Cathode Plasmas in Intense Relativistic Electron Beam Diodes," Ph.D. Thesis, MIT, 1984.
- 22) D. Mosher, (Private Communication)
- 23) J. W. Poukey, "Ion effects in relativistic diodes," Applied Physics Letters, Vol. 26, No. 4, 11, 15, pp. 145-146), February 1975.
- 24) D. S. Prono, H. Ishizuka, E. P. Lee, B. W. Stallard, and W. C. Turner, "Charge-exchange neutral-atom filling of ion diodes: its effect on diode performance and A-K shorting," J. Appl. Phys., Vol. 52, No. 4, pp. 3004-3011, April 1981.
- 25) Irving Langmuir, "The interaction of electron and positive ion space charges in cathode sheaths," Physical Review, Vol 33, pp. 954-989, June 1929.
- 26) R. K. Parker, R. E. Anderson, and C. V. Duncan, "Plasma-induced field emission and the characteristics of high current relativistic electron flow," J. Appl. Phys. 45, 2463 (1974).
- 27) D. Dakin and J. Benford, PI Memo, Oct. 1976